

2D Supramolecular Structures of a Shape-Persistent Macrocycle and Co-deposition with Fullerene on HOPG

Ge-Bo Pan,[†] Xiao-Hong Cheng,[‡] Sigurd Höger,^{*,‡} and Werner Freyland^{*,†}

Institute of Physical Chemistry and Institute for Technical Chemistry and Polymer Chemistry, Karlsruhe University, Kaiserstr. 12, 76128 Karlsruhe, Germany

Received January 20, 2006; E-mail: werner.freyland@chemie.uni-karlsruhe.de; hoeger@chemie.uni-karlsruhe.de

Self-organized systems have attracted considerable attention due to their potential applications in nanotechnology as a “bottom-up” approach for the construction of molecule-scale devices and nanostructures.¹ The organized objects can be molecular, macromolecular, supramolecular, and colloidal. Shape-persistent macrocycles are composed of a rigid molecular backbone and flexible (functional) side groups, which allow tailoring of new templates for self-assembly, and can be considered as promising building blocks.² By using nonspecific attractive interaction, one- and two-dimensional (1D and 2D) organizations have been obtained during the last years. On the other hand, highly ordered arrays of fullerenes are of particular interest from both the scientific and technological points of view and have been investigated on various substrates by using different methods.^{3,4}

Herein, we report the investigation of the 2D supramolecular structures of the shape-persistent macrocycle **1** and **1/C₆₀** (a two-component system) on HOPG under ambient conditions. Highly ordered arrays of **1** and **1/C₆₀** have been fabricated from 1,2,4-trichlorobenzene (TCB) by self-assembly and characterized by scanning tunneling microscopy (STM). In brief, a drop of TCB solution containing **1** (less than 1 mM) or **1/C₆₀** (1:4) was directly deposited onto the freshly cleaved surfaces of HOPG, dried in the Ar flow for about 2 h, and then transferred into a home-built airtight chamber for STM measurement.

Figure 1a represents a large-scale STM image of the (long range) ordered arrays of **1**. The angle between different domain directions is $120 \pm 2^\circ$, corresponding to the hexagonal graphite symmetry. The bright protrusion in the STM image is attributed to the unsaturated backbone of the macrocycles, whereas the dark stripes are occupied by the alkyl chains. This is the usual case that the aromatic and conjugated parts of the molecules show a higher tunneling probability than the aliphatic alkyl parts.⁵

A higher resolution STM image of **1** at the surface of the graphite is shown in Figure 1b. The macrocycles are organized into rows that are separated by the alkyl chains, which are interdigitated and oriented along one of the main symmetry axes of underlying HOPG lattice, maximizing their interaction with the substrate. The overall shape of the contrast of an individual macrocycle is qualitatively comparable with the electronic density of the highest occupied molecular orbital (HOMO), shown as an inset in Figure 1b. The four extraannular groups with oligo-alkyl side chains are also clearly visible and indicated with the green circles. These data strongly indicate that the rings are flat adsorbed at the graphite in order to maximize the compound/substrate interaction.⁶ On the basis of the analysis above, the parameters of an oblique unit cell were determined as $a = 3.6 \pm 0.2$ nm, $b = 5.0 \pm 0.2$ nm, and $\gamma = 70 \pm 2^\circ$. These values agree well with the calculated molecular sizes of **1** by AM1 method (see Supporting Information). Figure 1c shows

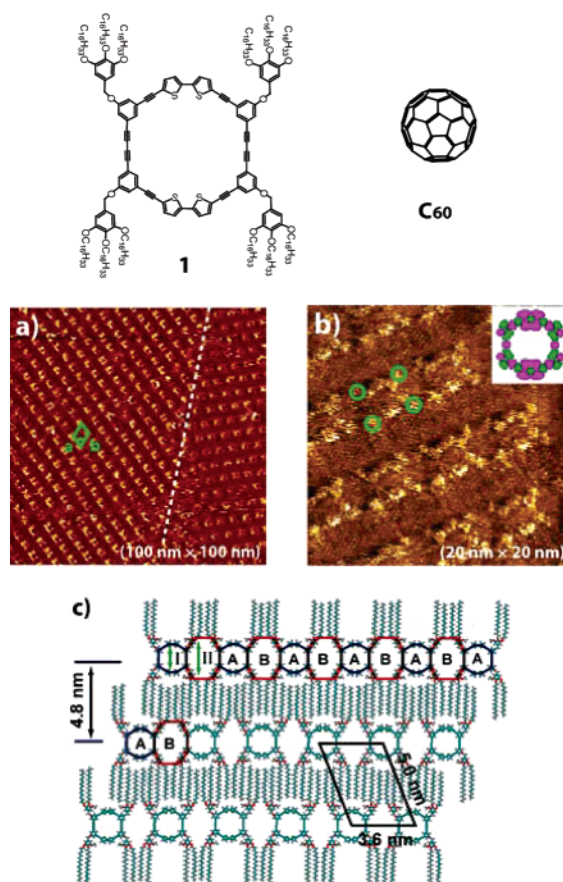


Figure 1. Ordered arrays of **1** on HOPG under ambient conditions. (a) Typical large-scale STM image. $V_{\text{bias}} = 0.35$ V; $I_t = 0.6$ nA. An oblique unit cell is indicated in green. (b) Higher resolution STM image. $V_{\text{bias}} = 0.41$ V; $I_t = 0.5$ nA. The four extraannular groups are indicated with green circles. The inset is the HOMO of the cyclic backbone of **1**. (c) Proposed structural model. The blue and red octagons indicate the two types of nanoscale holes, **A** and **B** (for large-size STM images, see Supporting Information).

a schematic model for the ordered arrays of **1**. Note that only two alkyl chains for each extraannular side group can be observed. The remaining alkyl chains are either directed to the air or adsorbed in a disordered fashion. Obviously, the structure contains the intrinsic empty holes **A** (blue octagon, ~ 1.4 nm) of the macrocycle as well as a second empty area **B** (red octagon, ~ 2.5 nm \times 1.8 nm). At present, it is not clear whether this empty space contains the remaining alkyl chains or not.

In addition to the investigation of the pure compound **1**, attempts have been made to self-assemble the two-component system of **1** and **C₆₀**. Fullerene–oligothiophene composites have attracted considerable attention during the past decade due to their remarkable electrooptical properties in organic solar cells.⁷ Figure 2a shows

[†] Institute of Physical Chemistry.

[‡] Institute for Technical Chemistry and Polymer Chemistry.

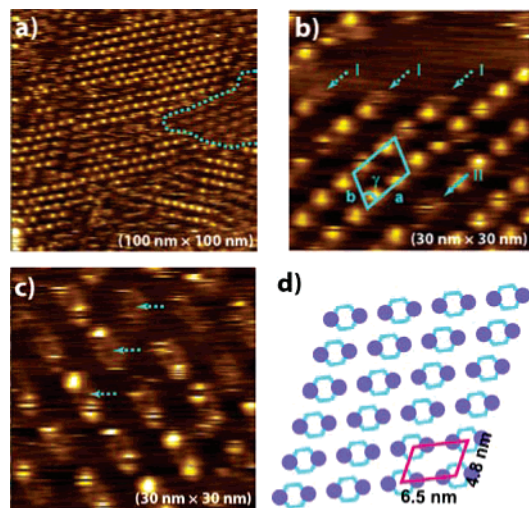


Figure 2. Ordered arrays of $1/C_{60}$ on HOPG under ambient conditions. (a) Typical large-scale STM image. $V_{\text{bias}} = 0.8 \text{ V}$; $I_t = 0.3 \text{ nA}$. (b) Higher resolution STM image. $V_{\text{bias}} = 1.0 \text{ V}$; $I_t = 0.3 \text{ nA}$. Arrows I and II indicate individual macrocycles. (c) Higher resolution STM image, revealing the adsorption site of C_{60} on the macrocycle. $V_{\text{bias}} = 1.0 \text{ V}$; $I_t = 0.3 \text{ nA}$. (d) Proposed structural model.

an example of the large-scale STM image. An interesting feature in the $1/C_{60}$ array are the well-ordered bright spots, which are significantly different from the pure **1** array discussed before. Each bright spot can be associated with an individual molecule of C_{60} . Note that these bright spots can be easily swept off during the continuous scanning without changing the imaging parameters, such as bias voltage and setpoint current. This last observation is indicative of the weak bonding between the C_{60} and macrocycle **1**. Careful inspection shows that areas of ordered bright spots are coexisting with small ordered domains of **1**.

Figure 2b and 2c shows higher resolution STM images acquired in the ordered $1/C_{60}$ array. Arrows I indicate the individual macrocycles, which are at the boundary of the ordered domain. For each macrocycle, two fullerene molecules can be detected. Arrow II indicates one defect in the ordered C_{60} array, where two bright spots are missing for an individual macrocycle. It is obvious that the bright spots are not located above the center of the macrocycle; that is, the C_{60} is not included in the intrinsic molecular hole (Figure 2c). Rather the C_{60} molecules are located at the two sides of the macrocycle. Therefore, the driving force for the formation of this superstructure is not the interaction of the C_{60} with the uncovered HOPG surface inside the rings but the donor–acceptor interaction between the C_{60} and thiophene groups.⁸

On the basis of the analysis above, an oblique unit cell (containing two C_{60}) is outlined in Figure 2b. The parameters are determined as $a = 6.5 \pm 0.2 \text{ nm}$, $b = 4.8 \pm 0.2 \text{ nm}$, and $\gamma = 75 \pm 2^\circ$, a significant difference in comparison to the pure **1**. Since C_{60} assembly has been observed only in co-deposition experiments, this structural change presumably is due to the donor–acceptor interaction of C_{60} and bithiophene units. Additionally, the nearest distance between the two fullerenes is measured to be $3.0 \pm 0.2 \text{ nm}$, which is consistent with the outside distance between the two bithiophene units of $\sim 2 \text{ nm}$ plus 0.7 nm for the C_{60} diameter. Figure 2d shows a tentative model for the ordered arrays of $1/C_{60}$. The purple circles represent the C_{60} molecules, while the cyan rings underneath are the macrocycles. In our experiments on $1/C_{60}$, we

have not succeeded in observing the alkyl chains due to their low contrast. Nevertheless, they should be located between the adjacent molecular rows and are interdigitated according to the lattice parameter.

In summary, two 2D supramolecular structures of macrocycle **1** and $1/C_{60}$ have been obtained on HOPG by self-assembly under ambient conditions and have been investigated by high-resolution STM. The monolayers of **1** are characterized by structures with perfect ordering over relatively large area. In the case of $1/C_{60}$, the size of the macrocycle **1** and the presence of two individual bithiophene units per ring lead in the final superstructure to a 1:2 stoichiometry. The fullerenes are not trapped at the graphite surface inside the macrocyclic holes but are located around the periphery of the bithiophene units. This clearly shows that the donor–acceptor interaction between C_{60} and the electron-rich units of the ring is the dominant factor for the structure formation. The as-prepared 2D supramolecular structures at present are used as a template for complex 3D structures.

Acknowledgment. This work was supported by Center of Functional Nanostructures at Karlsruhe University, DFG, and Fonds der Chemischen Industrie. G.-B.P. thanks the Alexander von Humboldt Foundation.

Supporting Information Available: Experimental methods, synthesis of macrocycle **1**, and large-size STM images. This material is available free of charge via the Internet at <http://pubs.acs.org>.

References

- (1) (a) Lehn, J. M. *Supramolecular Chemistry*; VCH: Weinheim, Germany, 1995. (b) Whitesides, G. M.; Boncheva, M. *Proc. Natl. Acad. Sci. U.S.A.* **2002**, *99*, 4769–4774. (c) Reinhoudt, D. N.; Crego-Calama, M. *Science* **2002**, *295*, 2403–2407. (d) Theobald, J. A.; Oxtoby, N. S.; Phillips, M. A.; Champness, N. R.; Beton, P. H. *Nature* **2003**, *424*, 1029–1031. (e) Eremtchenko, M.; Schaefer, J. A.; Tautz, F. S. *Nature* **2003**, *425*, 602–605.
- (2) (a) Moore, J. S. *Acc. Chem. Res.* **1997**, *30*, 402–413. (b) Grave, C.; Schlüter, A. D. *Eur. J. Org. Chem.* **2002**, 3075–3098. (c) Zhao, D.; Moore, J. S. *Chem. Commun.* **2003**, 807–818. (d) Höger, S. *Chem.—Eur. J.* **2004**, *10*, 1320–1329. (e) Yuan, Q.-H.; Wan, L.-J.; Jude, H.; Stang, P. J. *J. Am. Chem. Soc.* **2005**, *127*, 16279–16286. (f) Gong, J.-R.; Wan, L.-J.; Yuan, Q.-H.; Bai, C.-L.; Jude, H.; Stang, P. J. *Proc. Natl. Acad. Sci. U.S.A.* **2005**, *102*, 971–974.
- (3) (a) Sakurai, T.; Wang, X. D.; Xue, Q. K.; Hasegawa, Y.; Hashizume, T.; Shinohara, H. *Prog. Surf. Sci.* **1996**, *51*, 263–408. (b) Diederich, F.; Gomez-Lopez, M. *Chem. Soc. Rev.* **1999**, *28*, 263–277.
- (4) (a) Pan, G.-B.; Liu, J.-M.; Zhang, H.-M.; Wan, L.-J.; Zheng, Q.-Y.; Bai, C.-L. *Angew. Chem., Int. Ed.* **2003**, *42*, 2747–2751. (b) Theobald, J. A.; Oxtoby, N. S.; Phillips, M. A.; Champness, N. R.; Beton, P. H. *Nature* **2003**, *424*, 1029–1031. (c) Stepanov, S.; Lingensfelder, M.; Dmitriev, A.; Spillmann, H.; Delvigne, E.; Lin, N.; Deng, X.; Cai, C.; Barth, J. V.; Kern, K. *Nat. Mater.* **2004**, *3*, 229–233.
- (5) (a) Cyr, D. M.; Venkataraman, B.; Flynn, G. W. *Chem. Mater.* **1996**, *8*, 1600–1615. (b) Qiu, X. H.; Wang, C.; Zeng, Q. D.; Xu, B.; Yin, S. X.; Wang, H. N.; Xu, S. D.; Bai, C. L. *J. Am. Chem. Soc.* **2000**, *122*, 5550–5556. (c) De Feyter, S.; De Schryver, F. C. *Chem. Soc. Rev.* **2003**, *32*, 139–150.
- (6) (a) Höger, S.; Bonrad, K.; Mourran, A.; Beginn, U.; Möller, M. *J. Am. Chem. Soc.* **2001**, *123*, 5651–5659. (b) Borissov, D.; Ziegler, A.; Höger, S.; Freyland, W. *Langmuir* **2004**, *20*, 2781–2784. (c) Ziegler, A.; Mamdouh, W.; Heyen, A. V.; Surin, M.; Uji, H.; Abdel-Mottaleb, M. M. S.; De Schryver, F. C.; De Feyter, S.; Lazzaroni, R.; Höger, S. *Chem. Mater.* **2005**, *17*, 5670–5683.
- (7) (a) Chirvase, D.; Parisi, J.; Hummelen, J. C.; Dyakonov, V. *Nanotechnology* **2004**, *15*, 1317–1323. (b) Reyes-Reyes, M.; Kim, K.; Dewald, J.; Lopez-Sandoval, R.; Avadhanula, A.; Curran, S.; Carroll, D. L. *Org. Lett.* **2005**, *7*, 5749–5752.
- (8) (a) Swietlik, R.; Olejniczak, I.; Krol, S. *Fullerene Sci. Technol.* **1997**, *5*, 1243–1260. (b) Fomina, L.; Reyes, A.; Fomine, S. *Int. J. Quantum Chem.* **2002**, *89*, 477–483. (c) Borovkov, N. Y.; Blokhina, S. V.; Kutepov, A. M.; Lebedeva, N. S.; Pavlycheva, N. A. *Thermochim. Acta* **2005**, *430*, 167–171.

JA060469F